Numerical investigation of key parameters of the porous media combustion based Micro-Thermophotovoltaic system.

Stephen Bani [a,], Jianfeng Pan[a*], Aikun Tang[a] , Qingbo Lu[a], Yi Zhang[a]

[a] School of Energy and Power Engineering, Jiangsu University, Zhenjiang 212013, China

*Corresponding author: Prof. Jianfeng Pan

Address: School of Energy and Power Engineering, Jiangsu University, Zhenjiang 212013, China

Tel.: +86-0511-88780210

Fax: +86-0511-88780210

E-mail address: mike@ujs.edu.cn

Abstract

Power generation with porous media driven Micro-Thermophotovoltaic (MTPV) was investigated and effects of changes to key parameters of the system investigated. The micro combustor had the dimensions of length – 15 mm, width – 10 mm, height – 1 mm and wall thickness of 0.5 mm. The distance between the outside wall of combustor and the TPV cell was fixed at 1 mm. Variation in distance from 1 - 6 mm between the outside wall of the combustor and the thermophotovoltaic cell (TPV cell) caused a reduction of 13.75% and 1.4% in the radiation heat transfer efficiency and the TPV cell conversion efficiency respectively. An increase in the mixture flow rate from 300 mL/min to 1800 mL/ min caused an increase in the radiation heat transfer efficiency, TPV cell conversion efficiency and the total system efficiency. As the flow rate increased, the system's power output also increased. At 600 mL/min, the output power was 560 mW but rose to 3.2 W at the flow rate of 1800 mL/min. The cooling load of the system showed a linear growth as the flow rate increased. At 1800 mL/min the cooling load of the system was 12.4 W which is three times the cooling load at 900 mL/min.

Keywords: Thermophotovoltaic system, Radiation Energy, Micro-combustion, Porous media, Cooling load, Mixture flow rate.

1.0 Introduction

The proliferation of micro and nano devices have given birth to the miniaturization and multi fictionalization of micro-mechanical, communication, imaging, sensing, chemical analytical and biomedical devices [1, 2]. The devices so mentioned above need power sources that are portable, have short charging time, longevity, high energy density and are environmentally friendly. Chemical batteries hitherto used to be the major source of power for these devices but have a drawback of having low energy density. The most improved lithium-ion battery has energy density of about 0.2 kWh/kg [3]. Another problem of chemical batteries is the mode of disposal, which pose major environmental concern and they also have long charging time [4].

Combustion based power generators have been proposed as alternatives to the chemical batteries by using the advantages of hydrogen and hydrocarbon fuels. The combustion based micro-power generators have energy densities of about 12 kWh/kg, which is way above that of chemical batteries. The major concern is converting the vast chemical fuels into electricity in an efficient manner and in the millimeter scale [5] and also achieving uniform and high temperature distribution, a requirement for MTPV hence the need to optimize the micro combustor [6].

The main aim of optimizing the micro combustor is to attain uniform and high temperature distribution, a requirement for TPV conversion. This in effect improves total efficiency and performance of the MTPV system. The system's efficiencies are related as $\eta system = \eta combustor \cdot \eta filter \cdot \eta TPV$ and one can observe that the system efficiency is directly proportional to the combustor efficiency, hence the need for high combustor efficiency. The spectral radiance of a blackbody emitter working at 1500 K will be higher than that working at 1000 K [7]. This phenomenon is explained by the fact that radiation energy is proportional to the 4^{th} power of temperature and increase of emitter temperature also has the tendency of shifting the spectral radiance towards the short wavelength range. This occurrence is highlighted by Wien's displacement law. The peak spectral radiance is associated with a wavelength value in Wien's displacement law and multiplying this wavelength with the blackbody temperature gives a constant.

Various studies on the geometrical optimization of micro combustors have progressed over the years. As indicated earlier, a uniform distribution of temperature is ideal requirement for TPV generation. Ju et al. [1] opined that, increasing temperature of unburnt mixture has

the tendency of increasing the temperature of micro combustor walls hence increase combustion efficiency. Lee et al. [8] developed a micro combustor with heat recirculation to recycle thermal energy from exhaust of the combustor to preheat incoming fuel/oxidant mixture. The fuel/oxidant flows from a narrow channel into the combustor and the exhaust gas is expelled to the environment through the inner pipe. At the exhaust, the thermal energy from the hot gas is transferred to the walls of the pipe and the fresh fuel/oxidant mixture with the sole aim of increasing the combustion efficiency. A peak temperature of 1200 K at a flow velocity of 2.4 m/s was obtained at stochiometric condition and they also concluded that the temperature of the wall increased with increment in flow velocity. Zuo et al. [9] used numerical investigation of H_2/air premixed combustion in coflow and counterflow double channel and concluded that the outer wall temperature non-uniformity of counterflow setup is lower than the one with coflow. Fan et al. [10] used Swiss-roll combustor with bluff-body and said bluff-body can extend flame blow-off limit.

Park et al. [11] investigated combustion with heat recirculation and their studies actually concentrated on the consequence of variations in materials used for the combustor fabrication and also the void of TPV cell installed chamber. They concluded that, the combustor with silicone carbide (SiC) as material gave higher wall temperature than stainless steel as combustor material. They also found out that, the void of the TPV cell installed chamber had no major outcome on the working of the MTPV. Li et al. [12] conducted numerical studies on recirculation of heat in premixed H_2/air filtration combustion using micro planar combustor and said thermal conductivity of the solid matrix and porosity affects flame position and wall temperature.

In TPV power systems, radiant sources from combustion are used for power generation. The TPV cells change portions of the radiation energy emitted from the combustors into electrical power [13]. There should be a match between the bandgap of the TPV cell and the photo energy of the selected part of radiation. It is preferable to use TPV cells having low bandgaps since they make use of major parts of the radiation energy emanating from the combustor. A drawback is that, the efficiency of the cells may reduce to some extent if the bandgap is reduced as a result of decrease in fill factor and the open circuit voltage [14]. A major problem encountered with MTPV power generation is the mismatch between the radiation spectrum and the bandgap of the TPV cell. There is therefore the need to incorporate a high filter to mitigate the problem and also improve the system’s

performance. The combustor's spectral radiance is calculated by the blackbody radiance multiplied by the spectral emissivity of the reactor material[15].

The GaSb TPV cell has a cut-off wavelength of 1720 nm which implies the spectral radiance with wavelength lower than 1720 nm is only useful for power generation whiles the spectral radiance greater than 1720 nm is of no use. Various low bandgap TPV cells such as GaSb (0.72 eV) [16, 17], InGaAsSb (0.5-0.55 eV) [18, 19] and InAsSbP (0.45-0.48) [20] have been developed over the years. In order to meet the demands of the MTPV system with different bandgaps of TPV cells, the passband of the metamaterial filter should be tuneable and also have a wide band that maintains a high transmittance in relatively long wavelength range. When combustion occurs in the micro-combustor, the wall of the combustor starts to emit photons towards the hemisphere. The photons with the radiation energy within the passband of the metamaterial filter pass through while those out of the passband are reflected. The photons that pass through the filter are used for power generation while the reflected photons are useful for improving the temperature of the micro-combustor. However, a small amount of energy may be absorbed by the filter and emitted to the environment, resulting in energy loss. Therefore, the system efficiency is finally determined by the efficiencies of the combustor, filter and TPV cell [21].

Utlu et al. [22] studied the production of electricity by means of TPV using GaSb cells in the high waste heat temperatures and obtained highest spectral radiation at 3100 K. They also concluded among others that, the highest starting current density was 1.6 A/m^2 at 300 K source temperature. Bouzid and Dehimi [23] evaluated the performance of the GaSb thermophotovoltaic converter. It was evaluated under different levels of illumination. They concluded that radiator temperature near 2200 K is most advantageous and a reflectance of 0.98 was necessary for below bandgap irradiation to obtain conversion efficiency greater than 28% at 300 K cell temperature. Woolf et al. [24] demonstrated the use of a selective emitter at 1328 K for TPV power generation and opined that using a geometric view function of 24.1% of the radiation incident on the PV cell can be converted into electricity.

In spite of the vast and rich research works on the performance parameters of the TPV power generator enumerated above, many practical considerations for the use of porous media combustion (PMC) to further investigate the parameters are necessary. Due to the complex arrangement of the MTPV system, that is, coupling of combustion, heat transfer and photoelectric conversion, any change in the operating parameters of the system is likely to

have an effect on the general output and performance level of the system. It is convenient to refer to the energy conversion model established in our previous work [25]. This paper is dedicated to the study of generation of electricity using GaSb TPV cell in PMC, looked at the combustion performance of the H_2/O_2 fueled combustor and finally carried out preliminary calculations of the system to analyze influencing factors on the MTPV. The distance between the radiation wall and the TPV cell, the type of TPV cell and the radiation surface temperature will be of major concern in carrying out series of calculations to determine how the changes in these parameters will affect the system efficiency, power output among others to get the basic parameters for optimized system performance. The results will be practical for the design and improvement of MTPV power systems.

2.0 Micro combustor and experimental set up

The micro combustor applied in this work has the dimensions of 15 mm in length, 10 mm in width and 1 mm in height with the wall thickness being 0.5 mm. The micro combustor was inserted with stainless steel mesh having a porosity of 0.9. The combustor and flow connectors as depicted in fig.1 were made of 316L stainless steel. H_2/O_2 served as the fuel for the experiment and was supplied at an equivalence ratio of 1.0 and 0.8 respectively. The fuel enters the combustor through the inlet and the exhaust gas is expelled through the outlet after combustion.

The schematic diagram of the experiment is shown in fig. 2. Pressurized tanks supplied both hydrogen and oxygen with 99.99% purity at an outlet pressure of 0.15 MPa. The following were applied during the experiment:

Emissivity of wall – 0.8
Emissivity of solid matrix – 0.8
Conductivity of solid matrix – 16.27 W/mK
Ambient temperature – 293 K
Relative humidity – 76%

The mass flow controller, was used to set the inlet velocity and the equivalence ratio with the infrared thermal imager (Thermovision A40) having a focal length of 4 mm used to measure the wall temperature. It can detect temperature variations in the range of -40°C and 2000°C with accuracy of measurement being ±2%.

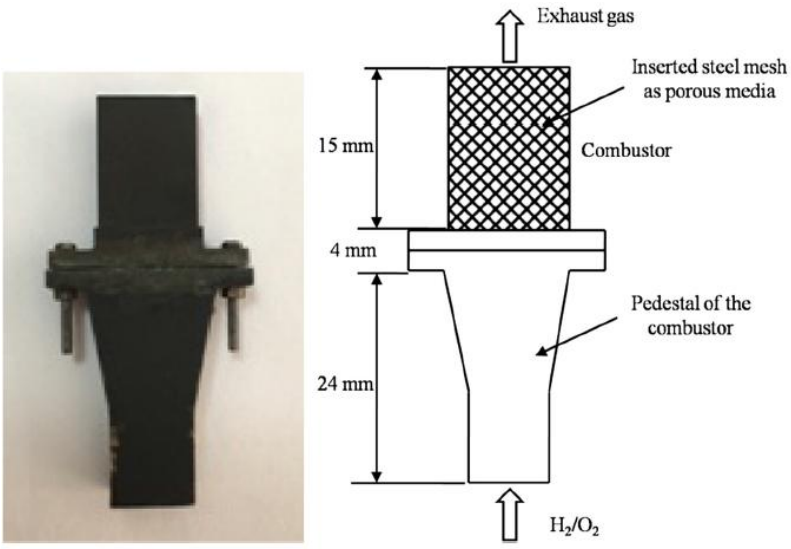

Fig. 1 (a) Photo of micro combustor, (b) design feature of the planar micro combustor and flow connector.

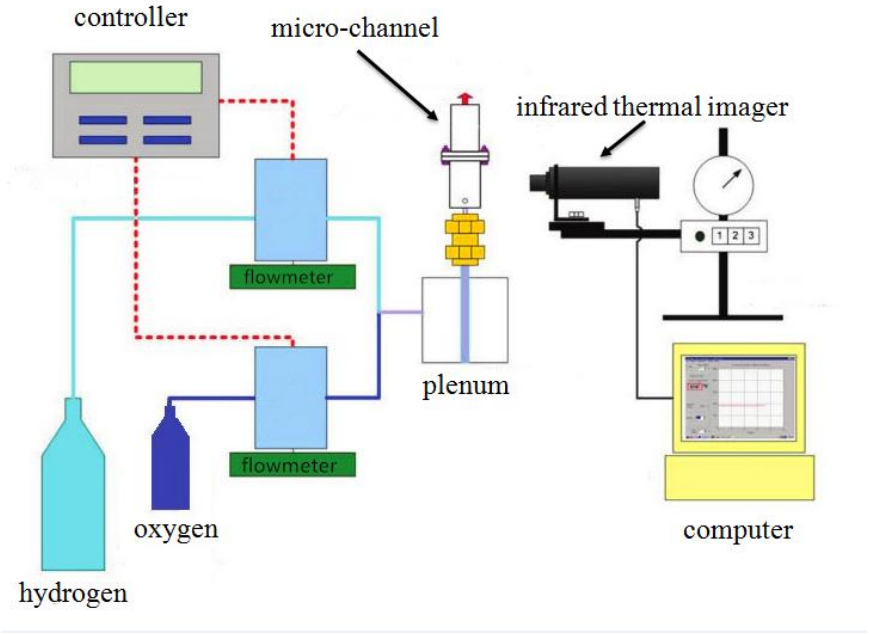

Fig. 2 Schematic of the experimental set-up.

3.0 Numerical models and simulation approach

The numerical model employed in this study was premised on a convectional combustor having a rectangular channel and the schematic diagram of the micro combustor, the wall of which was made of 316L stainless steel is as shown in fig.3. The whole combustion process begins with letting the premixed H_2/O_2 stream through the micro combustor.

It is quite a herculean task accessing the small space of the combustor with measuring devices. Thus a numerical approach was employed to study the H_2/O_2 premixed flame for exhaustive information in the combustor. A three dimensional (3D) simulation was carried out. A 3D uniform grid having three different mesh densities was developed. After checking the centerline gas temperature profiles of the three meshes as shown in fig. 4 it was concluded that the mesh with 0.1 mm in the x, y and z directions and having a total cell of 330,000 was best for the simulation.

The various walls of the micro combustor were designated with non-slip boundary conditions with initial temperatures set to 300 K for the combustion chamber, solid walls and also the temperature surrounding the combustion chamber.

The boundary conditions set for the inlet and the exit face were the velocity-inlet and outflow respectively. The H_2/O_2 equivalence ratio was 1.0 and 0.8 respectively.

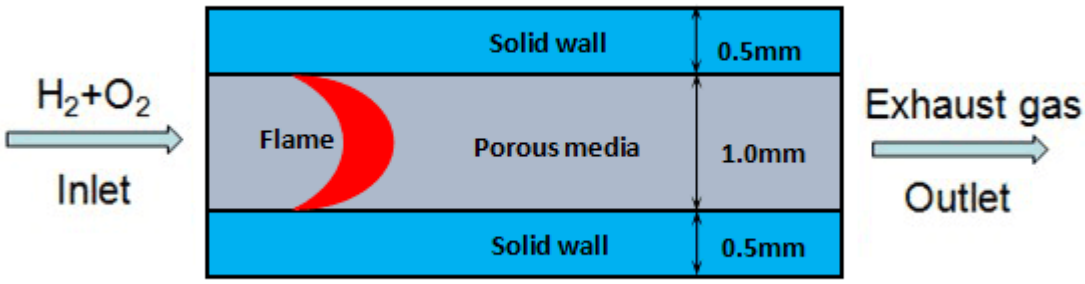

Fig. 3 Schematic of the computational domain.

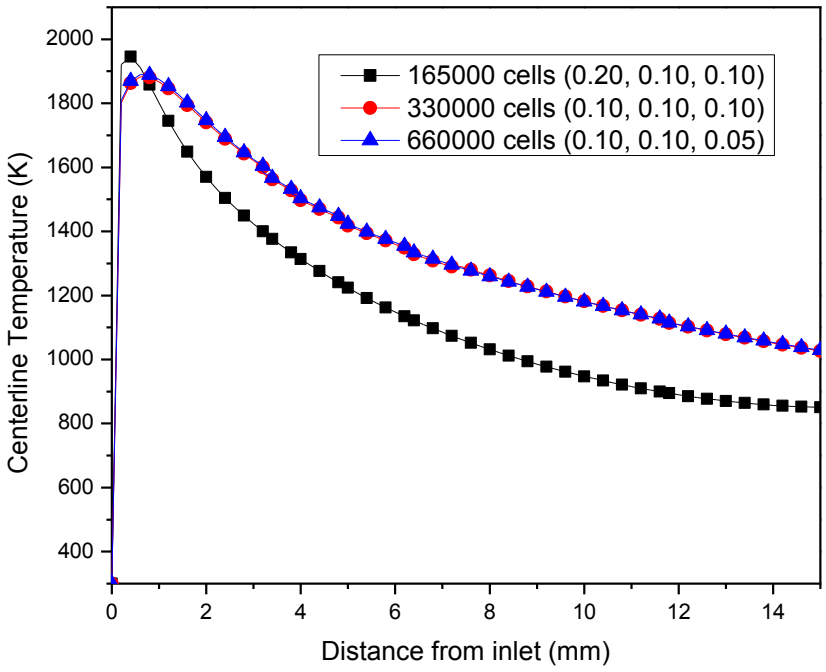

Fig.4 Distribution of the centerline temperature in the channel with different grid sizes under inlet velocity of 1.0 m/s.

The continuous flow was chosen for the mixture as the Knudsen number was less than 0.001. The RNG k-e turbulence model was adopted per the suggestion of Kuwahara et al. [26] to employ turbulence effect if Reynolds number is greater than 80 in porous medium (PM). EDC model was used to simulate the turbulence flow with complex chemical reaction mechanism. The radiation of the inner PM was dealt with using DO radiation model. At the combustor walls, mixed thermo boundary conditions were assigned. The inlet of the micro combustor had velocity boundary conditions specified; flow rate and mass fraction were also incorporated. A porous zone boundary condition was assigned to the fluid area and outflow boundary condition specified at the exit.

Permeability of PM, α and inertial resistance coefficients C_2 are given by Ergun equation:

$$\alpha = \frac{D_p^2}{150}\frac{\varepsilon^3}{(1-\varepsilon)^2} \tag{1}$$

$$C_2 = \frac{3.5}{D_p}\frac{(1-\varepsilon)}{\varepsilon^3} \tag{2}$$

Where D_{p} is average diameter of particles and ε is porosity of PM.

The following assumptions were made in coming up with the model: (1) Steady-state combustion, (2) no gas radiation, (3) no Dufour effects, (4) inert wall with no surface reactions, (5) the incorporated porous medium is isotropic and homogenous, (6) body forces are neglected, (7) no work done by pressure and viscous forces, and (8) detailed reaction mechanism applies. With the hindsight of the above assumptions, the governing equations for momentum, species, continuity and energy in PM are written as follows:

Continuity:

$$\nabla\cdot\left(\rho\bar{u}\right)=0 \tag{3}$$

Momentum:

$$\rho\left(\vec{u}\cdot\nabla\vec{u}\right)=-\nabla p+\nabla\cdot\left(\mu\left[\left(\nabla\vec{u}+\left(\nabla\vec{u}\right)^{T}-\tfrac{2}{3}\nabla\cdot\vec{u}I\right)\right]\right)-\left[\mu\left(\bar{D}\cdot\vec{u}\right)+\tfrac{p}{2}\|\vec{u}\|\bar{c}\cdot\vec{u}\right] \tag{4}$$

Energy:

$$\nabla\cdot\left[\vec{u}\left(pE_{\mathrm{f}}+p\right)\right]=\nabla\cdot\left[k_{\mathrm{eff}}\nabla T-\left(\sum\nolimits_{\mathrm{i}}h\bar{J}_{\mathrm{i}}\right)+\left(\mu\left[\left(\nabla\vec{u}+\left(\nabla\vec{u}\right)^{T}-\tfrac{2}{3}\nabla\cdot\vec{u}I\right)\right]\right)\cdot\vec{u}\right]+S_{\mathrm{f}}^{\mathrm{h}} \tag{5}$$

Where $k_{\mathrm{eff}}=\varepsilon k_f+\left(1-\varepsilon\right)k_s$ and S_f^h is the fluid enthalpy source term.

Species:

$$\nabla\cdot\left(\rho\bar{u}Y_i\right)=-\nabla\cdot\vec{J}_i+R_i+S_i \tag{6}$$

$$\vec{J}_i=-\rho D_{i\cdot\mathrm{m}}\nabla Y_i \tag{7}$$

The wall energy equation is written as:

$$\nabla\cdot\left(k_{\mathrm{w}}\nabla T\right)=0 \tag{8}$$

Heat lost to the surrounding from the external wall is given as:

$$q_{\mathrm{w}}=h\left(T_{\mathrm{w}}-T_{\mathrm{o}}\right)+\varepsilon_{\mathrm{w}}\sigma\left(T_{\mathrm{w}}^{4}-T_{\mathrm{o}}^{4}\right) \tag{9}$$

Where h is the heat transfer coefficient with a value of $10\ \mathrm{W/m^2K}$.

The RNG k-e turbulence model was used to deal with the flow whiles Finite-rate (mechanism comprising 8 species and 19 reversible reactions) was used to deal with the reaction. The conservation equations were discretized and solved numerically using the Simple solver in

fluent. The First-order upwind scheme was used to solve the governing equations since it gives faster convergence compared to other higher order schemes. The Simple algorithm was used to solve the pressure – velocity coupling. The momentum equations were first to be solved and this was immediately followed by the continuity equations and finally updating the pressure and velocity. The computational time was 30 hours for the 3D simulation using fluent and the simulation was deemed to have converged when the residuals of all governing equations were smaller than 10^{-6}.

4.0 Model validation

To confirm the accuracy of the numerical solution, we contrast the numerical simulation result with experimental data as shown in fig.5 from our previous work [25]. The distribution of temperature along the combustor wall shows a good agreement between the simulation and the experimental results hence confirming the accuracy of the model. The maximum deviation between the experimental results and the simulation were 2.7% and 2.4% for the equivalence ratios of 1.0 and 0.8 respectively.

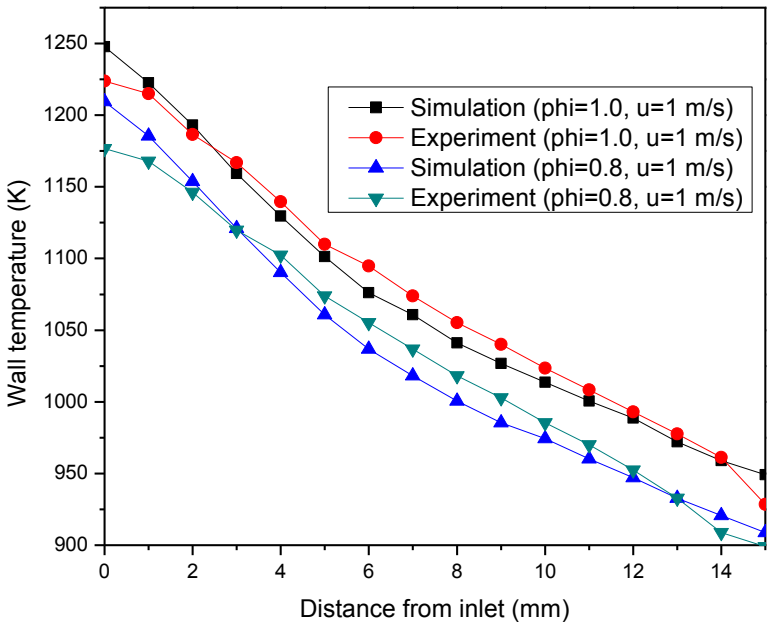

Fig. 5 Comparison of the external wall temperature distributions between the simulation results and experimental data.

5.0 TPV System Performance

This is estimated from temperature prediction and the TPV cell used is GaSb. A 1 mm distance was set between the TPV cell and combustor's external wall. A unique feature of the TPV cell is it gets hot in operation and therefore consented effort should be made to keep the temperature at 300 K. This is achieved by using cooling fins. The radiation wall temperature distribution is obtained from simulation using fluent software. A matlab code is developed to calculate the important performance parameters of the system.

The overall system efficiency is estimated as:

$$\eta_{\mathrm{TPV}} = \eta_{\mathrm{RS}} \cdot \eta_{\mathrm{RH}} \cdot \eta_{\mathrm{PV}} \tag{10}$$

Where η_{TPV} is total system efficiency, η_{RS} is combustion radiation efficiency, η_{RH} is radiation heat transfer efficiency and η_{PV} is PVC conversion efficiency.

The three efficiencies are given as:

$$\eta_{\mathrm{RS}} = \frac{\text{Net radiation of the side wall}}{\text{Chemical energy of fuel}} \tag{11}$$

$$\eta_{\mathrm{RH}} = \frac{\text{The usable radiation arrived at the PVC}}{\text{Net radiation of the side wall}} \tag{12}$$

$$\eta_{\mathrm{PV}} = \frac{\text{The electric Power output}}{\text{The usable radiation arrived at the PVC}} \tag{13}$$

The incident radiation of wall, P_{in} is given by [13]:

$$P_{\mathrm{in}} = \sum_{j=1}^{n} A(j) \cdot \int_0^{\infty} \varepsilon E_{\mathrm{b}\lambda}(j) d\lambda \tag{14}$$

Useful radiation P_{en} is cell energy band gap wavelength. It is derived as follows:

$$P_{en} = \sum_{j=1}^{n} A(j) \cdot C(j) \cdot \int_0^{\lambda g} \varepsilon E_{b\lambda}(j) d\lambda \tag{15}$$

Electric power P_{el} is given by:

$$P_{el} = V_{OC} \cdot FF \cdot J_{SC} \cdot A_{cell} \tag{16}$$

Where V_{oc} is open circuit voltage, FF is fill factor, J_{sc} is short circuit current density and A_{cell} is area of the TPV cell.

Short circuit current density is calculated by:

$$J_{sc} = \sum_{j=1}^{n} \frac{A(j) \cdot C(j)}{A_{cell}} \int_0^{\lambda g} \frac{E_{b\lambda} QE_{ext} q_0 \lambda}{hc} d\lambda \quad (17)$$

The V_{oc} is determined by Shockley formulation as:

$$V_{oc} = \sigma T_c \mathrm{In}\left(\frac{J_{sc}}{J_0} + 1 \right) \quad (18)$$

Where σ is Boltzmann constant, T_c is cell temperature and J_0 is saturation current density.

The saturation current density is estimated by [17]:

$$J_0 = 1.84 \times 10^3 \cdot T_c^3 \cdot \exp\left(-\frac{E_g q_0}{kT_c} \right) \quad (19)$$

Where E_g is energy bandgap, 0.72 eV for GaSb PVC.

Fill factor is calculated as:

$$FF = \frac{v - \mathrm{In}(v + 0.72)}{v + 1} \quad (20)$$

Where v is normalized V_{oc} calculated as:

$$v = V_{oc} q_0 / kT_c \quad (21)$$

6.0 Results and Discussions

6.1 The effect of spacing distance between external wall and TPV cell

For a conventional Photovoltaic system, the spacing between the radiation wall and the Photovoltaic cells is somewhat ignored since it has no effect on the system performance. The distance between the two walls can be approximately equal to 1 mm and there will not be any significant effect due to the spacing but spacing cannot be ignored in the case of micro combustion. When the spacing is increased by 1 mm, the angle coefficient between the two surfaces is significantly reduced resulting in the divergence of the radiation energy away from the face of the outer wall to the TPV cell. This means the photons reaching the TPV cell will be reduced. Therefore change in spacing will significantly affect the overall efficiency and power output. For the calculation process, the hydrogen to oxygen flow rate is 1800

mL/min at an equivalence ratio of 1.0. The size of the combustor and the TPV cell are kept the same, that is, 15 mm x 10 mm x 1 mm. The indicators of the energy conversion aspects of the evaluation system were defined earlier with no filter for combustion radiation efficiency, radiation heat transfer efficiency and TPV cell efficiency. The flow velocity of fuel to the combustor remains the same, therefore a change in spacing distance will not affect the combustion process of the porous burner and the output will not cause difference in the temperature of the radiation wall and total radiant energy. Therefore the combustion radiation efficiency will not change in each calculation. The effect of change in spacing is firstly analyzed on the radiation heat transfer efficiency and the TPV cell efficiency. As can be seen from fig. 6 both efficiencies show downward trend when the distance between the radiation wall and the TPV cell was adjusted from 1 mm to 6 mm. The change in the TPV cell efficiency is linear for any addition of 1 mm and this change is about 1.4%. There is obvious change in the radiation heat transfer efficiency. At the distance of 1 mm, the radiation heat transfer efficiency is 17.9% but it reduced to 8.5% when the spacing is 6 mm. This means with the same surface temperature, more radiation energy will be dissipated outside the TPV cell but the change is not linear.

Fig. 7 shows the output power and power density versus changes in spacing distance between the TPV cell and the radiation wall. The thickness of the cooling fin is ignored and the thickness of the GaSb single chip TPV cell is set to 0.65 mm. The output power is as shown in fig. 7 and is greatly influenced by the distance as it affects the radiation heat transfer efficiency. When the spacing is 1 mm, the output power is 2.7 W and the radiation heat transfer efficiency is 20.2% but as the distance increased to 6 mm, the output power reduced to 1.2 W and the radiation heat transfer efficiency reduced to 18.9%. As the distance decreases, the power density increases faster. At the spacing of 1 mm, the power density is 0.72 W/cm^3 but reduced to 0.32 W/cm^3 at 6 mm spacing. This demonstrates why high energy densities are advantages of the micro power system. From the above analysis, it can be observed that, as the distance between the external wall and TPV cell reduces, the system's performances are greatly improved and so there should be concerted effort to keep the distance between the radiating surface and the TPV cell at minimum. However, as the space decreases, more energy will be radiated to the TPV cell and thus produce more heat.

The cooling of the TPV cell is thus essential. Fig. 8 shows the cell's cooling load (two TPV cells) against spacing. When the distance between the external wall and the TPV cell is 1 mm, the cooling load of the cell is 10.6 W. There is the average reduction in the cell's

cooling load of about 1.1 W as the distance is adjusted from 1 mm to 6 mm. It can be observed that, if necessary measures are not taken to cool the TPV cells, their operating temperatures will increase and this intends affect the performance of the TPV system and hence reduction in the output power.

Table 1 Variation of key parameters with distance

Distance (mm)	TPV cell cooling Load (W)	radiation heat transfer efficiency (%)	TPV cell conversion efficiency (%)	Power Density	Output Power (W)
1	10.6179	17.9066	20.2768	0.7221	2.7006
2	9.0219	15.1609	19.9926	0.6028	2.2544
3	7.7456	12.9714	19.7158	0.5086	1.9021
4	6.7116	11.2026	19.4495	0.4333	1.6206
5	5.8601	9.7503	19.1935	0.3722	1.3919
6	5.1496	8.5421	18.9473	0.3219	1.2038

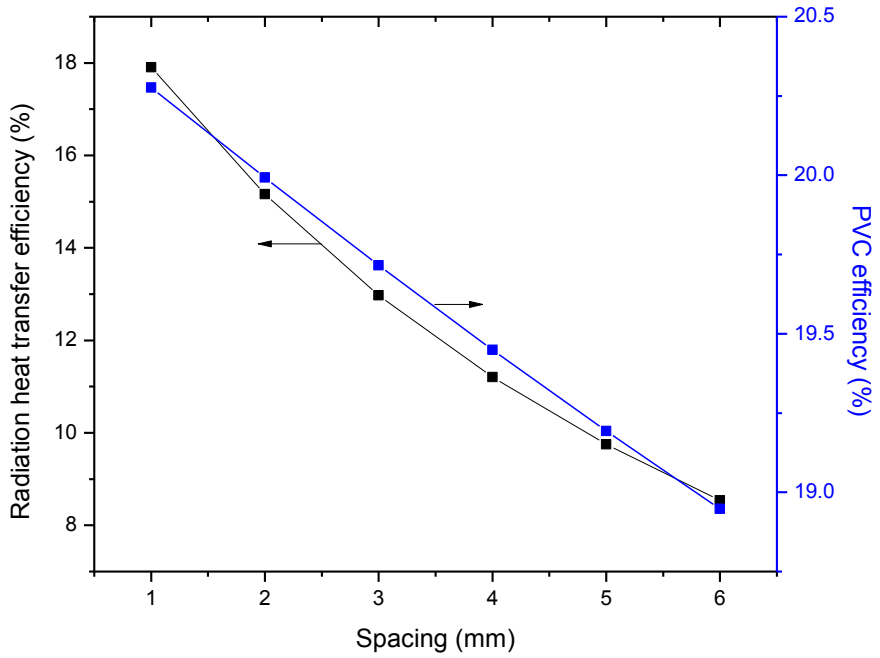

Fig. 6 Variation of radiation heat transfer efficiency and cell efficiency at different spacing distance.

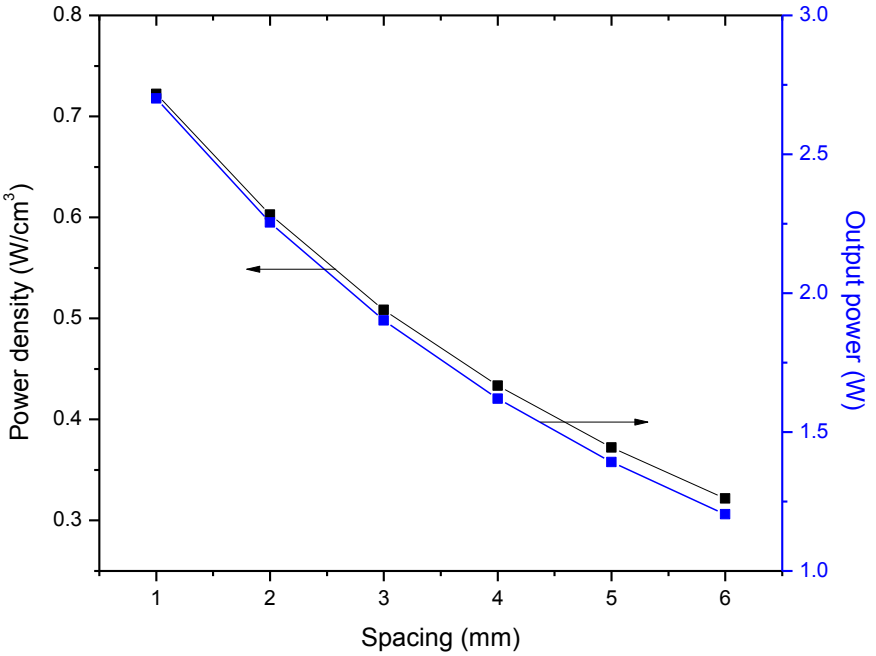

Fig.7 Variation of electricity output and volume power density at different spacing distance

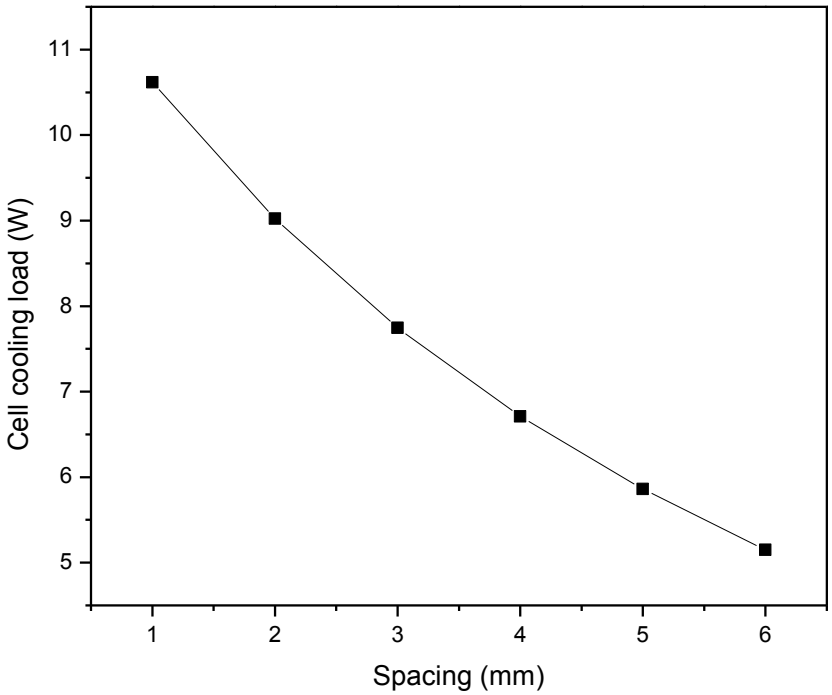

Fig.8 Variation of cell cooling load at different spacing distance

6.2 Radiation wall temperature distribution

From Planck's law, the radiated energy output power of the radiated surface of the thermoelectric system is proportional to its temperature to the 4^{th} degree. From the previous studies, we observed from both experiment and simulation that, as the mixture flow rate increases during combustion, the wall temperature is enhanced. Table 2 presents the MTPV system's efficiencies at different mixture flow rates. It is observed that, increment in the mixture flow rate leads to increase in the radiation heat transfer efficiency, TPV cell conversion efficiency and the total system efficiency. The most significant of all the increases is that of the radiation heat transfer efficiency. When the flow rate was 300 mL/min, the efficiency was only 6.81% but at 1800 mL/min, the radiation heat transfer efficiency was 18.69% an increase of about 63.5%.

It can be explained from figs 9 and 10 that, when the input fuel increases continuously, the total amount of internal energy absorbed by the combustion chamber also increases gradually leading to the enhancement of the overall temperature of the radiation surface.

This result in a significant increase in the amount of monochromatic radiation on the wall, where the amount of radiant energy that can be photo electrically converted increased at 300 mL / min when this part of the radiation in the total radiation energy share is less than 1%, while in the 1800mL / min when it reached 16%.

Table 2 Variation of each efficiency at different mixture flux

Mixed gas flow rate (mL / min)	chemical energy of Fuel (W)	Radiation surface average temperature (K)	combustion radiation efficiency η_{rs} (%)	radiation heat transfer efficiency η_{rh} (%)	PVC conversion efficiency η_{PV} (%)	system Total efficiency η (%)
300	42.5440	987.65	47.5639	6.8149	17.2244	0.5583
600	85.0879	1092.50	36.6334	9.7768	18.3859	0.6585
900	127.6319	1180.18	33.5329	12.3257	19.1459	0.7913
1200	170.1758	1260.44	32.6506	14.6378	19.7205	0.9425
1500	212.7198	1334.47	32.6232	16.7849	20.1764	1.1048
1800	255.2638	1404.03	32.9122	18.6925	20.5485	1.2642

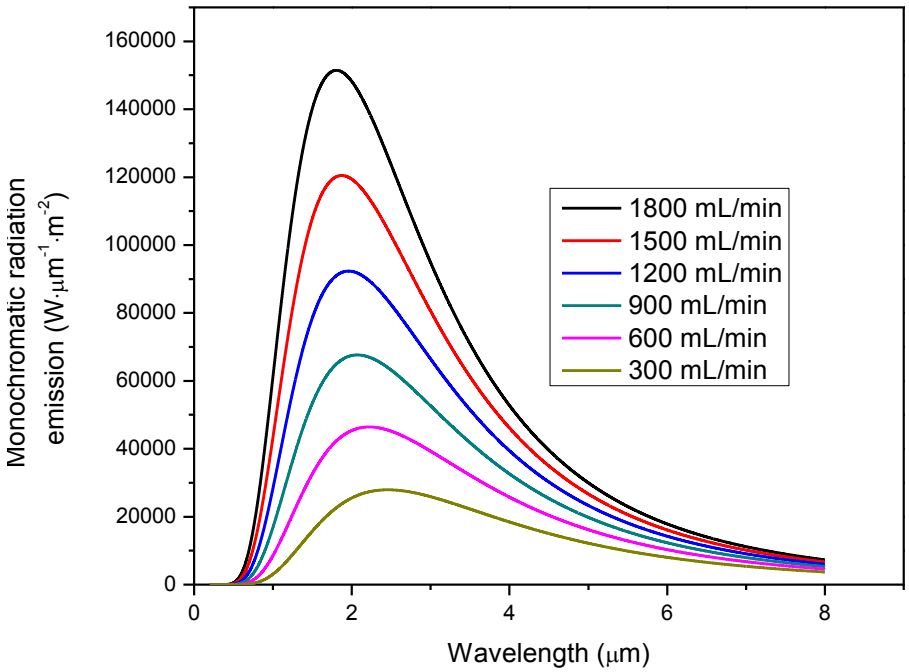

Fig. 9 Radiation energy spectrum distribution comparison at different mixture flux

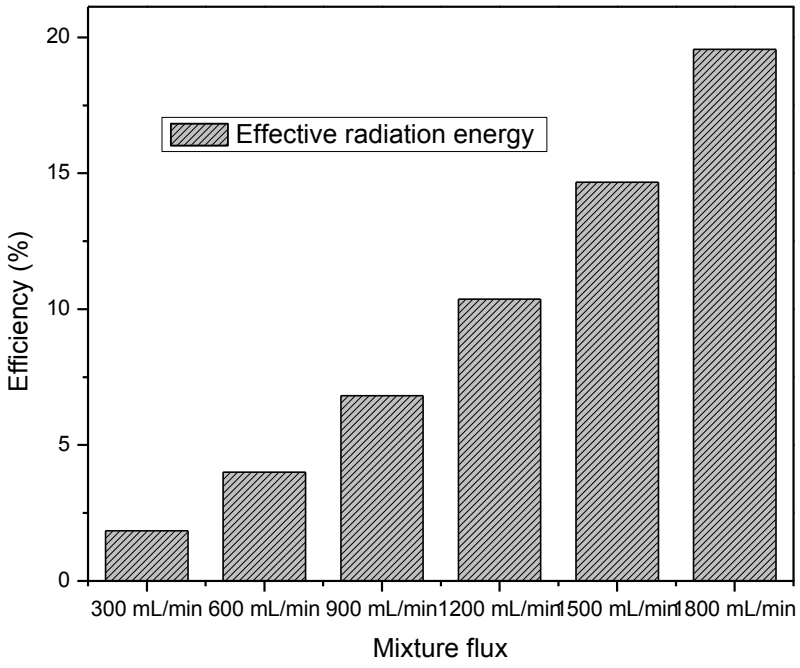

Fig.10 Effective radiation energy comparison at different mixture flux

It is also observed that, the increase in TPV cell conversion efficiency is more obvious in the low flow rate regime up to 900 mL/min but afterwards the amplitude witnessed a gradual increase due to the increase in the available portion of the radiation energy reaching the surface of the TPV cell. For the combustion radiation efficiency, we can see from Table 2 a very interesting phenomenon. At low flow rates, the variation in the combustion radiation efficiency witnessed an obvious reduction from 47.56% at 300 mL/min to 33.5% at 900 mL/min but between 900 mL/min and 1800 mL/min, there is not much change in the combustion radiation efficiency.

The speed of reduction in surface radiation cannot keep up with the pace of increase in input fuel. This shows that, when the flow rate of the mixture in the channel is too fast, the micro scale combustion process is carried out in a completely reduced degree.

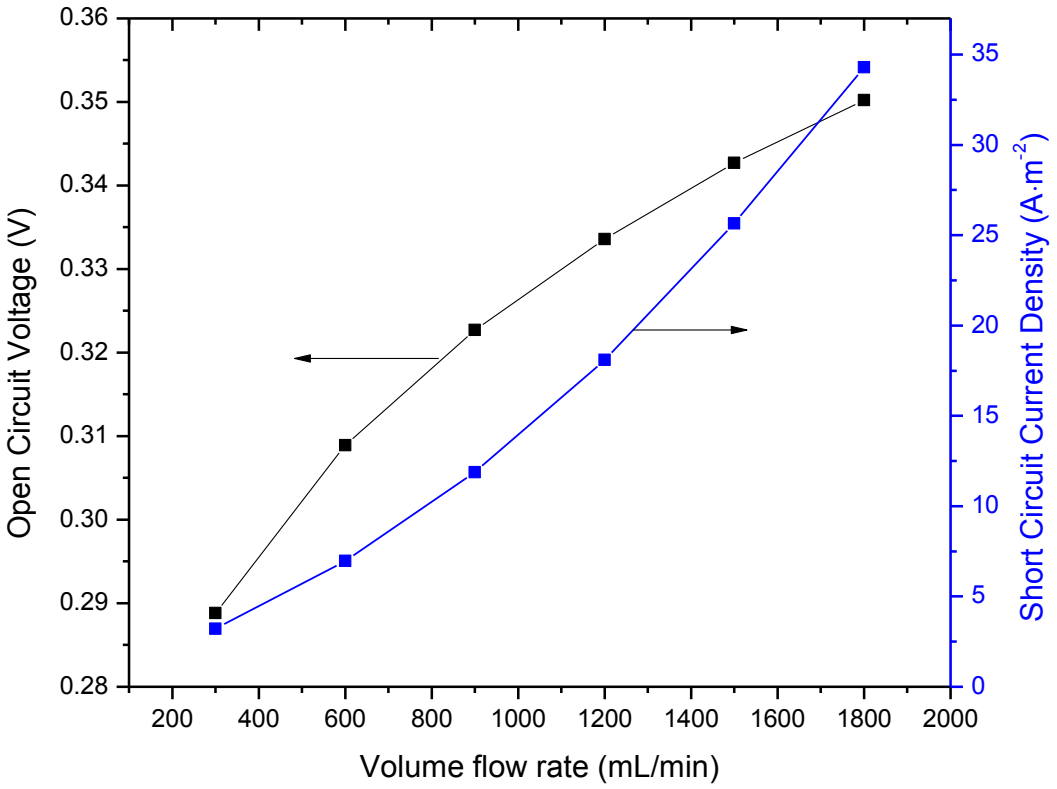

Fig. 11 Variation of short circuit current density and open circuit voltage at different mixture flux

Table 3 Variation of key parameters at different mixture flux

Mixture flow rate (mL/min)	Open circuit voltage (V)	Short circuit current density (A/m^2)	PVC cooling load (W)	Output power (W)
300	0.2888	3.21	1.1415	0.2375
600	0.3089	6.96	2.4872	0.5603
900	0.3227	11.87	4.2652	1.01
1200	0.3336	18.09	6.5294	1.6039
1500	0.3427	25.65	9.2979	2.3502
1800	0.3502	34.30	12.4772	3.227

The surface of the combustor can be used to improve the radiation energy of the system hence an increase in the open circuit voltage and short circuit current density. Fig.11 depicts the increase in open circuit voltage and short circuit current density. When the inlet flow rate was increased from 300 mL/min to 1800 mL/min, the open circuit voltage rose from 0.2888 V to 0.3503 V. The increase was much significant at the range 300 mL/min – 600 mL/min. The TPV cell conversion efficiency recorded changes in value as a result of the effect of the open circuit voltage on TPV cell conversion efficiency. The short circuit current density also experiences vast increment as compared to the open circuit voltage as the radiation surface temperature increases.

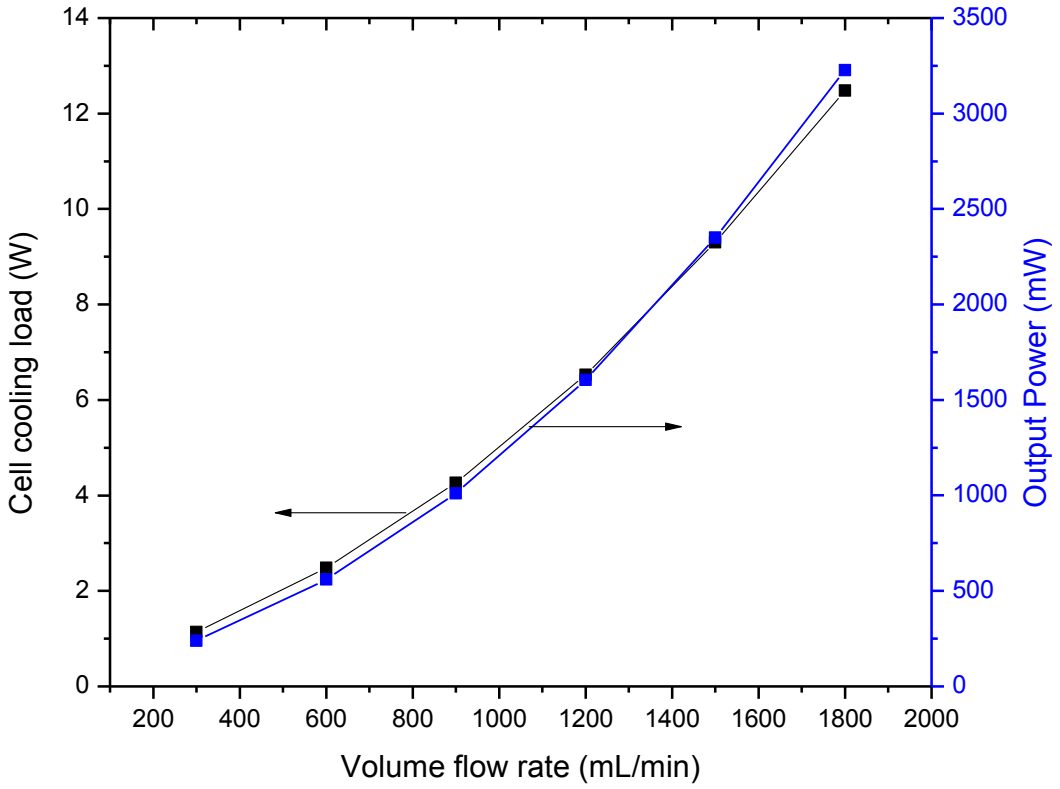

Fig.12 Variation of cell cooling load electricity output at different mixture flux

Fig.12 shows the effect of mixture flow rate on the cooling load and the output power of the system. It is observed that, though there was increase in the input fuel, there was significant increase in the total efficiency of the system. As the flow rate increases, the output power of the system also increases. At 600 mL/min, the output power of the system was 560.3 mW but rose to 3.2 W at the flow rate of 1800 mL/min. The increase in the input fuel makes the system able to meet the power requirement of different electromechanical devices. The increase in the temperature of the radiation surface will inevitably exacerbate the cooling burden of the TPV cells.

The cooling load of the system shows a linear growth as the flow rate increases. When the flow rate is 1800 mL/min, the cooling load of the system is 12.4 W which is three times the cooling load at 900 mL/min. Increasing the flow rate increases the surface temperature of the combustor hence great improvement in the entire system.

Also, as the intake fuel increases so also is the cooling burden imposed on the system. This shows that, great care should be taken in increasing the fuel in order to improve the radiation

surface temperature and also carefully select the right inlet flow rate range in order to augment the micro-scale combustion.

Conclusion

Numerical simulation of the energy conversion process in a micro combustor inserted with porous media having porosity of 0.9 for the application of MTPV systems was investigated. The performance of the entire system was estimated based on temperature prediction at the outer wall of the combustor obtained from fluent. A matlab code was developed to calculate key parameters of the system. The aim is to vary key parameters namely: variation of the distance between the TPV cell and the external surface of the combustor, vary the temperature of the TPV cell and also calculate the radiation surface temperature distribution of the system at different mixture fluxes. The performance of system was calculated and the following conclusions were made:

1. A change in distance has a huge effect on the performance of the TPV system. At a flow rate of 1800 mL / min and a distance between external wall and TPV cell ranging from 1 - 6 mm, the radiation heat transfer efficiency is reduced by 13.75 % for every 1 mm increase in distance, but the TPV cell conversion efficiency is only reduced by 1.4%.
2. At the distance 1mm the power output is 2.7 W and the power density is 0.72 W/cm3, but reduced to 1.2 W and 0.32 W/cm^3 at spacing 6 mm. When the distance decreases, the cooling of the TPV cell cannot be ignored, as there is an average reduction in the TPV cell cooling load of about 1.1 W as the distance is adjusted from 1 mm to 6 mm.
3. An increase in the mixture flow rate resulted in increase in the radiation heat transfer efficiency, TPV cell conversion efficiency and the total system efficiency. When the flow rate was 300 mL/min, the efficiency was only 6.8149% but at 1800 mL/min, the radiation heat transfer efficiency was 14.367%. Increasing the mixture flow rate enhances the overall temperature of the radiation surface and thus improves the performance of the MTPV system.

Acknowledgements

The authors acknowledge research grant from National Science Foundation of China (No. 51376082 and 51676088) and Project Funded by Priority Academic Program Development (PAPD) of Jiangsu Higher Education Institutions

Nomenclature

$A(j)$	Area of each element's surface, m^2
A_{cell}	Area of the PV cell, m^2
A_{in}	Area of combustor, m^2
C	Speed of light, $\mathrm{m/s}$
$C(j)$	Radiation angle factor between each element surface and the PV cell
C_2	Inertial resistance factor, m^{-1}
$\bar{d}$	Characteristic length scale of the pore, m
D_{p}	Average diameter of particles, m
E_{g}	Energy bandgap, eV
$E_{\mathrm{b}\lambda}(j)$	Spectral allocation of emissive power
FF	Fill factor
h	Planks constant, J/s
H	Width of the planar combustor, m
H_{fuel}	Heat value of fuel, J/kg
J_0	Saturation current density, $\mathrm{A/m}^2$
J_{sc}	Short circuit current density, $\mathrm{A/m}^2$
k_{w}	Thermal conductivity of wall, W/mK
k_{f}	Thermal conductivity of fluid, W/mK
k_{s}	Thermal conductivity of solid matrix, W/mK
k_{eff}	Effective bulk thermal conductivity of porous medium, W/mK
P_{in}	The incident radiation of the radiant wall, W
P_{rad}	Net radiation power emitted by the wall

P_{el}	The maximum electric power, W
P_{en}	The useful radiation, W
q_0	Elementary charge, C
QE_{ext}	External quantum efficiency
R_i	Rate at which species i is produced by chemical reaction
S_E	Emission area of emitter
S_i	Rate of creation as a result of adding from the dispersed phase
S_f^h	Fluid enthalpy source term, W/m^3
T	Temperature of the emitter, K
T_c	Cell temperature, K
u_{in}	Inlet velocity, m/s
$\bar{u}_p$	Mean pore velocity, m/s
V_{oc}	Open circuit voltage, V
V_s	Volume of the solid phase, m^3
V	Volume of the solid phase, m^3
W	Width of the porous medium, m

Greek Symbols

α	Permeability of porous medium, m^2
α_s	Thermal diffusivity of solid matrix, m^2/s
α_f	Thermal diffusivity of fluid, m^2/s
α_w	Thermal diffusivity of wall, m^2/s
ε	Porosity
ε_{wall}	Emissivity of combustor wall
η_{TPV}	Total efficiency of the system
η_{RS}	Combustion radiation efficiency
η_{RH}	Radiation heat transfer efficiency
η_{pv}	PV cell conversion efficiency
μ	Viscosity of fluid, $Pa \cdot s$

ρ	Density of fluid, $\mathrm{kg/m^3}$
σ	Stefan−Boltzmann constant, $5.67\times10^{-8}\ \mathrm{W/m^2\,K^4}$
ϕ	Equivalence ratio

Subscripts

f	Fluid
s	Solid matrix
w	Wall
$\bar{C}$	Inertia resistance, $\mathrm{m^{-1}}$
$\bar{D}$	Viscous resistance, $\mathrm{m^{-2}}$
$\vec{J}_i$	Diffusion flux of species i, $\mathrm{kg/m^2s}$
$\bar{u}$	Velocity vector, $\mathrm{m/s}$

Dimensionless Numbers

Bi	Biot number
Pe	Peclet number
Re_d	Reynolds number at pore scale

References

[1] Y. Ju and K. Maruta, "Microscale combustion: Technology development and fundamental research," *Progress in Energy and Combustion Science,* vol. 37, pp. 669-715, 2011.

[2] B. Fan, J. Pan, W. Yang, Y. Liu, S. Bani, and W. Chen, "Numerical investigation of the effect of injection strategy on mixture formation and combustion process in a port injection natural gas rotary engine," *Energy conversion and management,* vol. 133, pp. 511-523, 2017.

[3] K. Kang, Y. S. Meng, J. Bréger, C. P. Grey, and G. Ceder, "Electrodes with high power and high capacity for rechargeable lithium batteries," *Science,* vol. 311, pp. 977-980, 2006.

[4] S. Chou, W. Yang, K. Chua, J. Li, and K. Zhang, "Development of micro power generators–a review," *Applied Energy,* vol. 88, pp. 1-16, 2011.

[5] W. R. Chan, P. Bermel, R. C. Pilawa-Podgurski, C. H. Marton, K. F. Jensen, J. J. Senkevich, *et al.*, "Toward high-energy-density, high-efficiency, and moderate-temperature chip-scale thermophotovoltaics," *Proceedings of the National Academy of Sciences,* vol. 110, pp. 5309-5314, 2013.

[6] J. Pan, D. Wu, Y. Liu, H. Zhang, A. Tang, and H. Xue, "Hydrogen/oxygen premixed combustion characteristics in micro porous media combustor," *Applied Energy,* vol. 160, pp. 802-807, 2015.
[7] W. Yang, K. Chua, J. Pan, D. Jiang, and H. An, "Development of micro-thermophotovoltaic power generator with heat recuperation," *Energy Conversion and Management,* vol. 78, pp. 81-87, 2014.
[8] K. H. Lee and O. C. Kwon, "Studies on a heat-recirculating microemitter for a micro thermophotovoltaic system," *Combustion and Flame,* vol. 153, pp. 161-172, 2008.
[9] W. Zuo, E. Jiaqiang, Q. Peng, X. Zhao, and Z. Zhang, "Numerical investigations on a comparison between counterflow and coflow double-channel micro combustors for micro-thermophotovoltaic system," *Energy,* vol. 122, pp. 408-419, 2017.
[10] A. Fan, H. Zhang, and J. Wan, "Numerical investigation on flame blow-off limit of a novel microscale Swiss-roll combustor with a bluff-body," *Energy,* vol. 123, pp. 252-259, 2017.
[11] J. Park, J. So, H. Moon, and O. Kwon, "Measured and predicted performance of a micro-thermophotovoltaic device with a heat-recirculating micro-emitter," *International Journal of Heat and Mass Transfer,* vol. 54, pp. 1046-1054, 2011.
[12] J. Li, Q. Li, Y. Wang, Z. Guo, and X. Liu, "Fundamental flame characteristics of premixed H 2–air combustion in a planar porous micro-combustor," *Chemical Engineering Journal,* vol. 283, pp. 1187-1196, 2016.
[13] K. Qiu, A. Hayden, M. Mauk, and O. Sulima, "Generation of electricity using InGaAsSb and GaSb TPV cells in combustion-driven radiant sources," *Solar energy materials and solar cells,* vol. 90, pp. 68-81, 2006.
[14] P. Iles, C. Chu, and E. Linder, "The influence of bandgap on TPV converter efficiency," in *The 2nd NREL conference on thermophotovoltaic generation of electricity*, 1996, pp. 446-457.
[15] G. Neuer and G. Jaroma-Weiland, "Spectral and total emissivity of high-temperature materials," *International Journal of Thermophysics,* vol. 19, pp. 917-929, 1998.
[16] O. Sulima and A. Bett, "Fabrication and simulation of GaSb thermophotovoltaic cells," *Solar energy materials and solar cells,* vol. 66, pp. 533-540, 2001.
[17] L. Ferguson and L. Fraas, "Theoretical study of GaSb PV cells efficiency as a function of temperature," *Solar energy materials and solar cells,* vol. 39, pp. 11-18, 1995.
[18] O. Sulima, R. Beckert, A. Bett, J. Cox, and M. Mauk, "InGaAsSb photovoltaic cells with enhanced open-circuit voltage," *IEE Proceedings-Optoelectronics,* vol. 147, pp. 199-204, 2000.
[19] M. W. Dashiell, J. F. Beausang, H. Ehsani, G. Nichols, D. M. Depoy, L. R. Danielson, *et al.*, "Quaternary InGaAsSb thermophotovoltaic diodes," *IEEE Transactions on Electron Devices,* vol. 53, pp. 2879-2891, 2006.
[20] A. Popov, V. Sherstnev, Y. Yakovlev, R. Mücke, and P. Werle, "High power InAsSb/InAsSbP double heterostructure laser for continuous wave operation at 3.6 μm," *Applied physics letters,* vol. 68, pp. 2790-2792, 1996.
[21] M. Zenker, A. Heinzel, G. Stollwerck, J. Ferber, and J. Luther, "Efficiency and power density potential of combustion-driven thermophotovoltaic systems using GaSb photovoltaic cells," *IEEE Transactions on Electron Devices,* vol. 48, pp. 367-376, 2001.
[22] Z. Utlu and B. S. Önal, "Performance evaluation of thermophotovoltaic GaSb cell technology in high temperature waste heat," vol. 307, p. 012075, 2018.
[23] F. Bouzid and L. Dehimi, "Performance evaluation of a GaSb thermophotovoltaic converter," *Revue Des Energies Renouvelables,* 2012.

[24] D. N. Woolf, E. A. Kadlec, D. Bethke, A. D. Grine, J. J. Nogan, J. G. Cederberg, *et al.*, "High-efficiency thermophotovoltaic energy conversion enabled by a metamaterial selective emitter," *Optica,* vol. 5, p. 213, 2018.
[25] S. Bani, J. Pan, A. Tang, Q. Lu, and Y. Zhang, "Micro Combustion In A Porous Media For Thermophotovoltaic Power Generation," *Applied Thermal Engineering,* 2017.
[26] F. Kuwahara, T. Yamane, and A. Nakayama, "Large eddy simulation of turbulent flow in porous media," *International Communications in Heat and Mass Transfer,* vol. 33, pp. 411-418, 2006.